A datacentric long term rockburst intensity prediction for underground excavations

Ruffin Ntumbo Ya Leza Kayembe
Department of Civil Engineering Science, University of Johannesburg, Johannesburg, South Africa, and
Maria Ferentinou
School of Civil Engineering and the Built Environment, Liverpool John Moores University, Liverpool, UK

Abstract

Purpose – Rockbursts are characterised by the sudden and violent ejection of rock fragments due to the spontaneous release of strain energy stored within the rock mass. They are more frequent in deep underground excavations and high-stress zones. Although, rockbursts have long been the subject of extensive research, and valuable insights have been gained over time, they continue to present a persistent challenge in underground excavation projects. In this context, the present study aims to establish a mapping relationship between rock burst intensity and contributing factors.

Design/methodology/approach – A data set was compiled of 254 rockburst instances from published experimental results. Each occurrence was characterised by six critical variables: maximum tangential stress (σ_θ); uniaxial compressive strength (σ_c); uniaxial tensile strength (σ_t); brittleness index B1 (σ_θ/σ_c); brittleness index B2 (σ_c/σ_t); and strain energy storage index (W_{ET}).

Findings – Multi perceptron autoencoder models were developed to assess the performance of the neural network, and the potential of the data set to support data centred long term rock burst intensity prediction.

Originality/value – The results were evaluated through confusion matrices and four accuracy measures for data mining multiclass problems including accuracy, precision, recall and F1-score and receiver operating characteristic curve, suggesting that perceptron autoencoder model achieved a promising success rate of 85.8%.

Keywords Tunnelling and underground spaces, Geohazards: risk assessment and mitigation,
Predictive modelling: analysis of geotechnical data and automated classification

Paper type Research paper

1. Introduction

Deep underground excavations have long been subjected to numerous geotechnical hazards, especially in highly stressed environments. These hazards not only compromise the safety of personnel but also significantly slow down operational activities and result into property damage, casualties and other severe consequences (Cortés *et al.*, 2024; Tian *et al.*, 2025). Rockbursts can occur at both shallow and deep depths, depending on ground stress conditions and are typically characterised by the sudden, uncontrolled ejection of rock fragments, resulting in ground instability affecting deep mines and tunnels (Cortés *et al.*, 2024). Factors contributing to the manifestation of rockbursts, are *in situ* stress regime, the mechanical and physical properties of the surrounding rock mass, the structural features of the rock mass such as joints, faults and bedding planes, as well as ground water conditions like pore water pressure and groundwater flow (Fan *et al.*, 2024). The effect of construction, such as excavation methods, blasting intensity, excavation rate and the sequence of tunnelling or mining operations can significantly influence the likelihood and severity of rockburst occurrences (Feng *et al.*, 2012; Cai, 2024; Li *et al.*, 2025). The complex interaction of these geological and operational factors makes rockburst prediction a challenge in rock engineering (Lv *et al.*, 2024; Ren *et al.*, 2025).

Despite the development of numerous methods aimed at assessing and predicting rockburst occurrences in deep underground excavations (Li *et al.*, 2025), many of these approaches are based on the principles of *in situ* observations, empirical formulas, numerical simulations and analytical methods and have proven to lack effectiveness in terms of plausible practical solutions (Cortés *et al.*, 2024; Wang *et al.*, 2024), often fail to capture the dynamic behaviour of rock masses under high stress conditions and are unable to generalise well across different geological settings (Salmi and Sellers, 2021; Wang *et al.*, 2024).

The primary challenge lies in the highly complex and non-linear nature of rockburst phenomena, which are influenced by multiple

The current issue and full text archive of this journal is available on Emerald Insight at: **https://www.emerald.com/insight/3029-0414.htm**

Machine Learning and Data Science in Geotechnics
1/1 (2025) 109–123
Emerald Publishing Limited [ISSN 3029-0414]
[DOI 10.1108/MLAG-04-2025-0014]

Received 29 April 2025
Revised 7 June 2025
Accepted 21 August 2025

interacting geological, geomechanical and environmental factors (Askaripour *et al.*, 2022). Data-driven environment, particularly artificial intelligence and machine learning techniques seem to be plausible alternatives to address the inherently non-linear characteristics of rockburst phenomena, as they have complex structures themselves, they can encode information about their environment in a distributed form, that allows learning from historical data and adapt to complex underground conditions with enhanced precision and reliability, even when the data are inaccurate and incomplete (Cortés *et al.*, 2024; Wang *et al.*, 2025).

Notable, documented rockburst cases include the Kolar gold mine in India, the site of the world's first documented rockburst incident in 1900. Other instances of rockbursts were observed in the Sudbury region of Canada during the 1950s. Several copper-nickel mines experienced a series of rockburst with magnitudes reaching 3.8. These incidents highlighted the persistent threat posed by rockbursts in mining operations. Between 1984 and 1985, Ontario mines documented a staggering 217 rockburst occurrences with a magnitude of 4.0, which ultimately led to the closure of affected mines. The well-known Witwatersrand gold mines in Gauteng, South Africa, hosted several rockbursts, including those at the City Deep mine in April 1928 and at the Simmer and Jack mines in 1936. The period from 1984 to 1993 saw a significant escalation in rockburst incidents, with 680 documented occurrences in 31 gold mines across South Africa. Tragically, these incidents resulted in the loss of 3,275 workers' lives (Hedley, 1987; Blake and Hedley Rockbursts, 2003).

2. Contributing factors controlling rockburst manifestation

Rockburst mechanism is primarily characterised by the accumulation of stress in the rock mass surrounding an underground opening (Rong *et al.*, 2024; Wang *et al.*, 2025; Li *et al.*, 2025). When this stress exceeds the rock's strength threshold, often due to changes in boundary conditions, excavation-induced stress redistribution or the presence of geological discontinuities, the rock may fracture suddenly and violently, resulting in a rapid release of stored strain energy (Cai, 2024; Fan *et al.*, 2024; Li *et al.*, 2025). The sudden release of strain energy generates seismic shockwaves that propagate through the surrounding rock mass, potentially resulting in structural damage and the high-velocity ejection of rock fragments into the excavation (Chen *et al.*, 2024; Jiang *et al.*, 2025; Watson *et al.*, 2025). Rockburst occurrences can vary significantly in terms of type, triggering mechanisms, intensity and resulting damage (Cai, 2024; Li *et al.*, 2025). While rockbursts are commonly associated with high *in situ* stress environments, they can also occur under relatively low-stress conditions, depending on the geological setting and excavation methods (Cai, 2024).

In geological formations subjected to high vertical stress, increasing depth leads to greater overburden pressure exerted by the overlying rock layers (Lei *et al.*, 2025). This vertical stress accumulation can exceed the strength of the rock mass, resulting in violent fracturing and energy release, hallmarks of rockbursts (Wu *et al.*, 2024). Conversely, in geological formations dominated by high horizontal stress, the rock layers are primarily subjected to lateral forces. These forces can lead to deformation mechanisms such as buckling or folding (Ren *et al.*, 2025). Such structural failures can also result in specific types of rockbursts, particularly in brittle rock formations where horizontal stress surpasses the rock's ability to resist deformation (Rong *et al.*, 2024).

Geological factors encompass the lithological characteristics of the rock, as well as the structural configuration of the rock mass (Qi *et al.*, 2024). Mining and excavation activities play a critical role in the triggering mechanisms of rockbursts (Chen *et al.*, 2024; Hu *et al.*, 2024). Factors such as the excavation method, blasting intensity, extraction rate and overall mining layout can significantly disturb the natural stress equilibrium within the rock mass (Du *et al.*, 2024; Zhou *et al.*, 2024a, 2024b). High extraction rates and insufficient ground support, particularly in deep mining operations, often lead to unstable stress redistribution around underground openings, thereby increasing the likelihood of rockburst occurrences (Cai, 2024; Witkowski *et al.*, 2024). Seismic activity, both natural earthquakes and mining-induced tremors, can also trigger rockbursts (Moein *et al.*, 2023; Witkowski *et al.*, 2024). These seismic events send stress waves through the rock mass, disrupting the equilibrium and potentially initiating or accelerating existing cracks. Even small vibrations can cause significant failures in rocks already near their stress limits (Zhou *et al.*, 2024a, 2024b). Hydrogeological conditions contribute to the instability of underground excavations (Fan *et al.*, 2024). Gas pressure within the rock mass can exacerbate rockburst risks (Shan *et al.*, 2024). The accumulation of high-pressure gases such as methane or carbon dioxide in deep rock layers can act as an additional force when suddenly released, intensifying the magnitude of a burst. In some cases, this gas release can itself trigger or accompany the mechanical failure (Wang *et al.*, 2024).

Ortlepp and Stacey (1994) classified rockbursts based on their damage mechanisms into four types:

1. strainburst;
2. rock buckling;
3. rock ejection; and
4. arch collapse, illustrated in Figure 1.

Kaiser *et al.* (1996) introduced the source and the damage mechanism.

3. Overview of commonly used machine learning methods in rockburst prediction

Machine learning (ML) classifiers, such as support vector machines (SVM), random forests (RF) and decision trees (DT), have been applied to rockburst prediction due to their capability to model complex, nonlinear relationships in geotechnical data. Table 1 summarises an overview of commonly used machine learning methods for rockburst intensity prediction. Notably, Wojtecki *et al.* (2024) demonstrated the effectiveness of ensemble learning for hazard estimation in coal mines, highlighting improved generalisation compared to single-model approaches. Miao *et al.* (2024) enhanced the performance of RF classifiers by integrating Boruta feature selection, which improved both the accuracy and robustness of rockburst risk prediction models. Another study used SVM for kimberlite burst prediction, achieving an accuracy of 95% (Pu *et al.*, 2019). These models rely on key

Figure 1 (a) Strainburst, (b) buckling, (c) ejection and (d) collapsed arch schematic

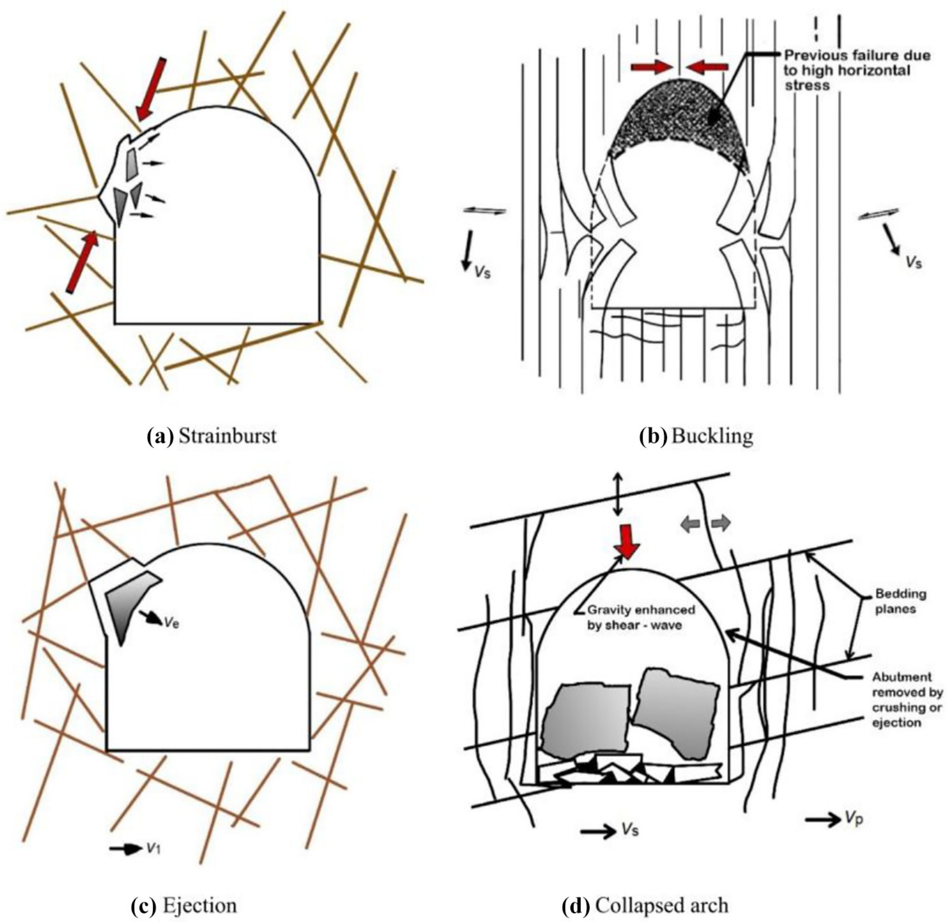

Source: Figure courtesy of Ortlepp and Stacey (1994)

indicators such as rock stress coefficient, brittleness coefficient and elastic energy index to construct the prediction system.

Hybrid ML models, which combine optimisation algorithms with classifiers, have also shown promise in improving predictive performance. Zhou *et al.* (2023) explored hybrid models such as particle swarm optimisation SVM (PSO-SVM), Harris Hawks optimisation SVM (HHO-SVM) and moth flame optimisation SVM (MFO-SVM), with the latter achieving a classification accuracy of 95.59%. Luo *et al.* (2023) reported that stacking ensemble techniques significantly outperformed individual classifiers, while Jia *et al.* (2024) used an arithmetic optimisation strategy to combine seven classifiers, yielding a 4.4% improvement in predictive accuracy compared to the best standalone model.

Deep learning models have gained traction for their ability to autonomously learn abstract features from raw input data. Convolutional neural networks (CNNs) have shown strong potential in structured geotechnical applications. Li *et al.* (2023) proposed a Bayes-optimised CNN that outperformed conventional methods in rockburst prediction, especially in data sets with hierarchical spatial features. Mahmoodzadeh *et al.* (2024) further demonstrated the capacity of deep learning models to generalise across diverse geological settings by incorporating kinetic energy-based inputs derived from simulation data.

The eXtreme gradient boosting (XGBoost) algorithm has also been applied to predict rock burst intensity, showing improved performance over SVM and RF. The integration of SHapley Additive explanations (SHAP) values into XGBoost models has allowed researchers to identify and quantify the influence of critical variables on rockburst occurrence (Chen *et al.*, 2023). Furthermore, Lin *et al.* (2024) proposed a framework combining variational autoencoders with NGBoost, which not only addresses class imbalance – a common issue in rockburst data sets but also enhances interpretability by producing probabilistic feature importance scores.

4. Data sources

4.1 Compilation of the data set

The data set used in this paper is a compilation of 254 published worldwide rockburst manifestation events from Zhou *et al.* (2012) (108), Xia *et al.* (2022) (82), Xu *et al.* (2022) (18) and Dong *et al.*, (2013) (46). The data involve several underground engineering projects such as mines, tunnels, hydropower chambers and nuclear power stations. The

Machine Learning and Data Science in Geotechnics
Volume 1 · Number 1 · 2025 · 109–123

Table 1 Overview of commonly used machine learning methods

Authors	Method	Data set		Findings	Range of application	Limitations
Chen *et al.*, 2023	XGBoost + SHAP	341 cases worldwide	σ_θ, σ_c, σ_t, SCF, (stress concentration factor), B = σ_c/σ_t, wet	High prediction performance; W_{ET} and σ_θ critical factors	Global hard rock projects	SHAP interpretation required
Jia *et al.*, 2024	AOA-Voting-Soft Ensemble (7 classifiers)	Rockburst datasets	σ_θ, σ_c, σ_t, B1, B2, Wet	Ensemble increased prediction by 4.4%	Underground projects	Complex ensemble process
Li *et al.*, 2023	Bayes optimised CNN (BOCNN)	Jiangbian hydropower station	σ_θ, σ_c, σ_t, B1, B2, Wet	BOCNN showed robust and generalised performance	Underground projects	Specific to structured datasets
Lin *et al.* (2024)	VAE + NGBoost + XAI (SHAP, anchor)	537 rockburst cases	T_{max}, σ_c, σ_t, wet, D (burial depth), shear strength coefficient C (the ratio of the maximum tangential stress To the uniaxial compressive strength	VAE-NGBoost improved imbalanced dataset classification; explainability added	General mining	Complex model training
Miao *et al.* (2024)	Boruta-RF, Boruta-GBM, SVM, KNN	118 cases (coal mining)	Mining depth, coal thickness, dip angle, bursting liability, structure, situation of goaf, mining face layout, roof management, pressure relief, safety management system, risk evaluation, rock burst hazard, operation or command violations, security monitoring and warning, rockburst prevention, on-site supervision and management	Boruta feature selection improves model accuracy	Coal mining	Limited to certain feature sets
Mahmoodzadeh *et al.* (2024)	Various ML models (6 types)	300 datasets from Abaqus simulations	σ_x: Horizontal stress; σ_z: Vertical stress; r: Tunnel radius; θ: weak plane angle; d: weak plane location respected to tunnel; l: weak plane length; ρ: Density; ν: poisson ratio Poisson's ratio; E: Young's modulus; UCS: Uniaxial compressive strength; ϕ: Friction angle; c: Cohesion; μ: friction coefficient; kmax: Kinetic energy; vmax: Ejection velocity	Weak planes and kinetic energy critical for rockburst	Deep tunnel construction	Synthetic data
Zhou *et al.* (2023)	LDA, QDA, PLSDA, NB, KNN, MLPNN, CT, SVM, RF, GBM	246 rockburst events	Seismic data base	RF and GBM outperformed others	General underground projects	Depends on input variable selection
Wojtecki *et al.* (2024)	ANN, decision tree, random Forest, GBM	Hard coal mines (Poland), 627 cases	Seismic data base, InSAR displacement mapping	Ensemble models performed best; ANN slightly leading	Coal mines	Small dataset, limited geography

Source(s): Table by authors

geographical extend of the data set is China, Norway, Japan, Sweden and spans a wide lithological record from sedimentary, to igneous ad metamorphic rocks. A diverse and wide data set ensures that it sufficiently represents the problem through training examples, so that the developed machine learning models can adequately generalise.

An extract of the data set is presented in Table 2, including rockburst prediction variables, namely, (σ_θ) which refers to the tangential stress around underground opening, (σ_c) refers to the uniaxial compressive strength, (σ_t) refers to the uniaxial tensile strength; (W_{ET}) refers to the strain energy storage index used to quantify the capacity of a material to store and release elastic strain energy Kidybiński (1981). The data base also contains, data on the rock brittleness indices B1 (Russenes, 1974), which is the ratio of the maximum shear stress (σ_θ) to the uniaxial compressive strength (σ_c) of the rock material. A higher B1 value indicates a higher susceptibility of the rock to brittle failure. It suggests that the rock is more likely to experience shear fracturing and sudden failure under applied stress (Jia *et al.*, 2024). Rock brittleness indices B2: is calculated as the ratio of the uniaxial compressive strength (σ_c) to the uniaxial tensile strength (σ_t) of the rock material. A higher B2 value indicates a lower brittleness of the rock material. It suggests that the rock has a higher capacity to withstand tensile stress and deformation without fracturing. In this study, the database was classified into four grades of rockburst intensity according to damaging grades (no, weak, moderate, strong), (Zhou *et al.*, 2012).

Table 2 Rockburst data set

Case no.	Rock type	σ_θ (MPa)	σ_c (MPa)	σ_t (MPa)	$B1 = \sigma_\theta/\sigma_c$	$B2 = \sigma_c/\sigma_t$	W_{ET}	Rockburst intensity
1	Granite porphyry	26.9	62.8	2.1	0.42	29.9	2.4	Moderate
	Diorite	24.93	99.7	4.8	0.28	20.7	3.8	No
2	Rhyolite	60	135	15.04	0.44	8.97	4.86	Moderate
3	Rhyolite	40.4	72.1	2.1	0.56	34.33	1.9	Moderate
...	...	...	...	...	...	...	...	...
254	Granite	68	107	6.1	0.63	17.54	7.2	Strong

Source(s): Table by authors

4.2 Statistical analysis

Descriptive statistics, of the data set: the minimum and maximum values, mean, total number of observations, standard deviation, are summarised in Table 3. The data exhibit considerable variability, particularly in σ_c (std = 53.92), σ_θ (std = 31.78) and B2 (std = 13.17) values. In contrast, B1 and W_{ET} energy values are relatively lower and more consistent.

Figure 2 presents the distribution of the rockburst parameters, and interclass distribution, which clearly demonstrates that there are outliers in the database, that can affect the predictive performance of the ML model but also show the wide variability of rock mass properties.

The visualisation in Figure 3 serves to depict the relationships between the different rockburst indicators and their respective statistical distributions. The off-diagonal plots show corelations between the variables, whereas the diagonal plots show the distribution of the variable per rockburst grade. From the visual inspection of the pair scatter plots there are few linear correlations between input parameters. A correlation between σ_c and intensity rank is identified, as well as σ_t and intensity rank.

In this study, the database was classified into four ranks according to damaging grades 0, 1, 2 and 3, which represent incidents of no (20.5%), weak (24.4%), moderate (39.4%) and strong rockburst (15.7%), respectively. The frequency and distribution are summarised through Figure 4. The rockburst intensity level was categorised using standard classification criteria (Zhou *et al.*, 2012) outlined in Table 4. In this case a binary variable for each category was applied following a natural ordering between categories. In this case, “no rockburst” was encoded as [1 0 0 0]; “moderate rockburst” was encoded as [0 1 0 0] and so on.

5. Machine learning modelling

5.1 Data pre-processing normalisation

Data normalisation was applied to scale the numerical values without distorting their original distribution, while preserving essential information. The MinMaxScaler function from the scikit-learn library in Python was used for this purpose. Partitioning the data set into three distinct groups, namely, training data, validation data and testing data, holds great significance for the effective development and evaluation of machine learning models. This division allows for a systematic approach to model building, fine-tuning and assessment. Typically, the data set is divided into a ratio of 70% for training data, 15% for validation data and 15% for testing data, although these proportions may vary depending on the specific requirements of the problem and the available data (Xu and Goodacre, 2018). After the division, there were 60 sets of sample data in the training set and the training set was used to train the neural network model and update the parameters. There were 15 sets of sample data in the test set, and the test set was used to evaluate the generalisation ability of the model and test the real prediction accuracy of the model.

5.2 Multilayer perceptron (MLP) autoencoder model

Bengio *et al.* (2007) introduced a method for training deep neural networks using a greedy, layer-wise unsupervised pretraining strategy. Each layer is trained as an autoencoder to learn compressed representations of its input, and successive layers are stacked on top, forming a deep neural network architecture. After unsupervised pretraining, the entire network is fine-tuned using supervised learning. This approach

Table 3 Descriptive statistics of the rock burst dataset

Statistic	σ_θ (MPa)	σ_c (MPa)	σ_t (MPa)	$B1 = \sigma_\theta/\sigma_c$	$B2 = \sigma_c/\sigma_t$	W_{ET}
Count	254.00	254.00	254.00	254.00	254.00	254.00
Mean	55.15	120.82	7.09	0.44	22.12	5.23
Std	31.78	53.92	4.77	0.20	13.37	4.06
Min	2.60	18.32	0.38	0.05	0.15	0.85
25%	31.25	80.15	3.25	0.31	13.12	2.89
50%	50.28	118.74	6.00	0.42	21.22	4.88
75%	69.80	152.65	9.26	0.57	27.63	6.24
Max	167.20	306.58	22.60	1.05	80.00	30.00

Source(s): Table by authors

Figure 2 Distribution of Rockburst variables and interclass distribution

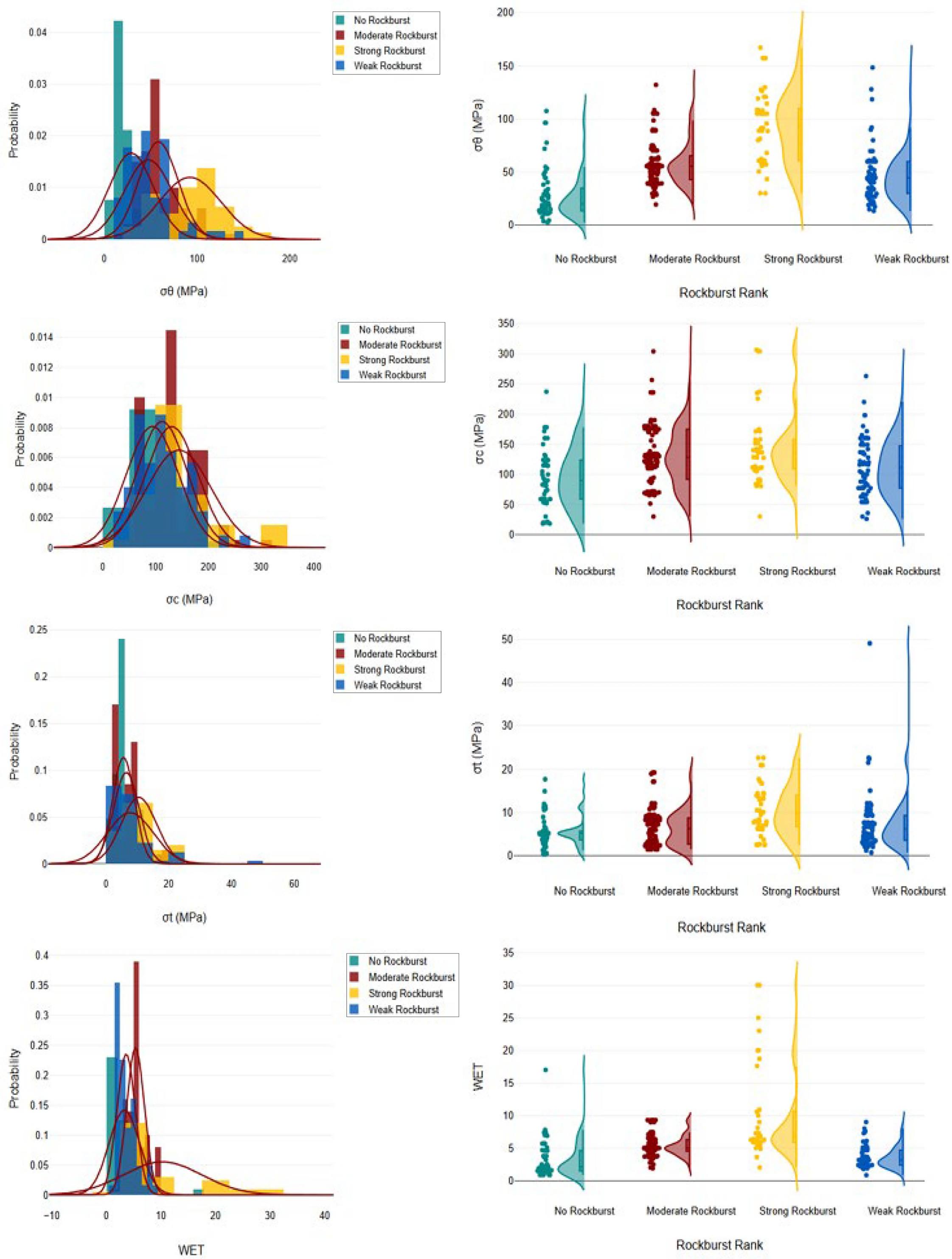

Source: Figure by authors

mitigated issues like vanishing gradients and poor convergence that plagued traditional deep networks.

Networks' architecture illustrated in Figure 5, included a two layered feedforward network with six features as input, representing the rockburst variables and four output targets, corresponding to output rockburst grades (Figure 4). The activation function used in the hidden layers is the sigmoid function:

Figure 3 Scatter plot correlation between input and output parameters

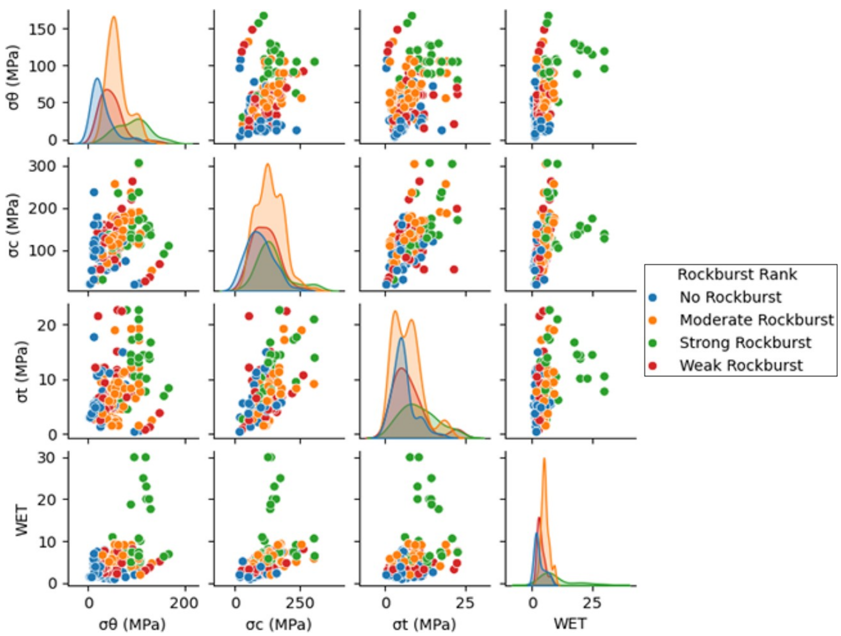

Source: Figure by authors

Figure 4 (a) Frequency of rockburst incidents by rockburst class; (b) pie chart of rockburst incidents

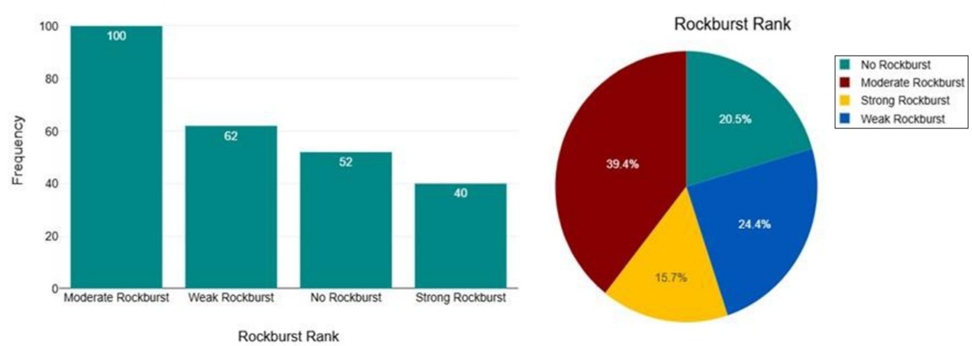

Source: Figure by authors

Table 4 Standard for rockburst intensity classification

Rockburst grade	Meaning	Failure characteristics
1 0 0 0	None rockburst	There is no sound of rock burst or rockburst activity
0 1 0 0	Weak rockburst	The surrounding rock is spalled, cracked or stripped and there is a weak sound but no ejection phenomenon
0 0 1 0	Moderate rockburst	The surrounding rock is more severely deformed and fractured with a considerable amount of rock chip ejecting, loose and sudden destruction, accompanied by a crunchy squeak which often appears in local cavern in the surrounding rock
0 0 0 1	Strong rockburst	The surrounding rock bursts severely and suddenly thrown or shot into the tunnel, accompanied by strong bursts and roaring sounds, air jets, the continuity of storm phenomena and the rapid expansion into deep surrounding rock

Source(s): Table by authors, adopted from Zhou *et al.* (2012)

Figure 5 Multilayer perceptron (MLP) autoencoder model architecture

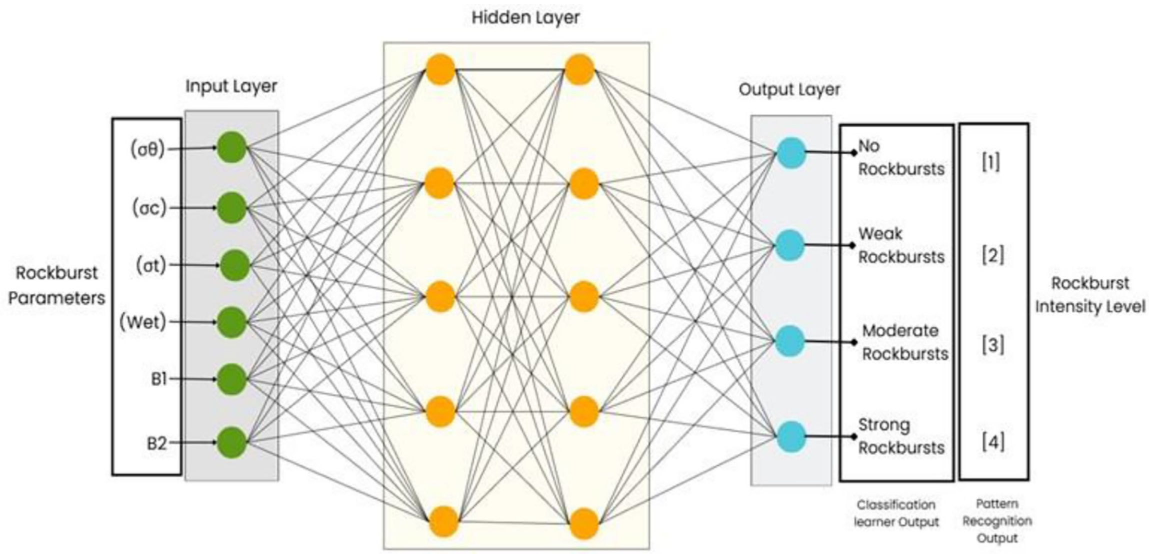

Source: Figure by authors

$$\sigma(x) = \frac{1}{1 + e^{-X}} \tag{1}$$

This function introduces non-linearity and allows the network to capture complex relationships and patterns within the data. The output function used is the SoftMax function, which is commonly used for multi-class classification problems:

$$SoftMax(x_i) = \frac{e^{xi}}{\sum_{j=1}^{N} e^{xj}} \tag{2}$$

The artificial neural network models were designed to predict four output classes corresponding to rockburst intensity levels: 1 (no), 2 (weak), 3 (moderate) and 4 (strong) rockburst. Design modelling was conducted to examine the influence of input parameters on the target output and to identify the best-fitting response surface model for the data set, using the optimal feature combination. Subsequently, the developed neural network models were trained, tested and evaluated. The developed models included the independent stress parameter and energy strain factor considering the four input variables (σ_θ, σ_c, σ_t, W_{ET}), for Model 1, and subsequently added the B1, Model 2, B2 Model 3 and (σ_θ, σ_c, σ_t, B1, B2, W_{ET}), Model 4, to test the importance of the input variables in the performance of the models. Data splitting percentage was set to 80% training and 20% testing (Model 5) to test the effect of data splitting percentage in the model performance. The input parameters, layer size and model performance is presented in Table 5. The obtained error rates for the best performing network Model 4 were as follows: 92.7% for training; 76.3% for validation; and 63.2% for the test data set, as summarised in Table 7.

The neural network model attained its peak performance at epoch 50. Both the gradient descent optimisation, which minimises cross-entropy, and the cross-entropy values displayed diminishing trends, approaching zero as training progressed. The cross-entropy error, which measures the disparity between the predicted probability distribution and the actual distribution, was used as another performance indicator. The gradient descent is an optimisation algorithm used here to minimise the cross-entropy error. At the optimal model, the gradient descent reached 0.0625, while the cross-entropy error corresponding performance was 0.05, signifying successful convergence with minimal disparity between predicted and actual observations, as presented through Table 6 and Table 7. These values indicate a successful convergence of the model as they approach 0, which signifies a minimal discrepancy between predicted and actual distributions. It highlights the model's high adaptability to the provided data set, suggesting

Table 5 Comparison of neural network models' performance

	Feature selection	Data splitting	Layer size	Training (%)	Validation (%)	Test (%)	Overall (%)
Model 1	(σ_θ, σ_c, σ_t, W_{ET})	70% Training/30% Test	20	77.0	65.8	71.1	74.4
Model 2	(σ_θ, σ_c, σ_t, B1, W_{ET})	70% Training/30% Test	50	83.7	60.5	60.5	76.8
Model 3	(σ_θ, σ_c, σ_t, B2, W_{ET})	70% Training/30% Test	80	80.9	78.9	63.2	78.0
Model 4	(σ_θ, σ_c, σ_t, B1, B2, W_{ET})	70% Training 30% Test	150	92.7	76.3	63.2	85.8
Model 5	(σ_θ, σ_c, σ_t, B1, B2, W_{ET})	80% Training/20% Test	200	89.9	80.2	60.3	83.5

Source(s): Table by authors

Table 6 Training progress

Unit	Initial value	Stopped value	Target value
Epoch	0	56	1,000
Elapsed time	–	00:00:06	–
Performance (cross-entropy)	4.44	0.05	0
Gradient (scaled conjugate)	2.25	0.0695	1e−06
Validation check	0	6	6

Source(s): Table by authors

Table 7 Best-performing neural network Model4 performance

Process	Total rockburst observations (254)	Optimiser: cross-entropy	Error rate
Training	178 (75%)	0.0625	0.0730
Validation	38 (15%)	0.2759	0.2237
Test	38 (15%)	0.2251	0.3684

Source(s): Table by authors

that it has effectively learned and captured the underlying patterns.

Figure 6 displays the progression of the gradient descent curve and the validation loss (Val fail) during training. The curve shows a consistent downward trend, indicating a reduction in errors and an enhancement in the model's accuracy across iterations. Furthermore, the evolution of the validation loss (Val fail) across epochs during validation checks is depicted in lower Figure 6 plot, assessing the model's performance on separate batches of validation data. To address overfitting, the data set is divided into multiple batches or k-folds, with six batches used in this instance.

Figure 7 illustrates the progression of training, validation and testing curves. The training curve (blue) shows the most significant drop, indicating minimal error and highest accuracy during training compared to validation and testing. The best validation performance peaks at epoch 56 with a cross-entropy value of 4.44. In contrast, the training curve (blue) reaches its optimal performance at epoch 50 with a cross-entropy value of 0.14245. This gap highlights the delicate balance between model complexity and overfitting, underscoring the importance of epoch selection for effective training and generalisation.

6. Results

6.1 Confusion matrix

The confusion matrix is a tool for evaluating the performance of classification models. It provides insights into how well the model distinguishes between different classes by categorising predictions into true positives (TP), true negatives (TN), false positives (FP) and false negatives (FN). Rockburst intensity prediction is a common multiclassification problem in data mining, the results of the classification were assessed with five common evaluation metrics, including precision, recall, F1 score, accuracy, receiver operating characteristic (ROC) curve. The calculation formula for each evaluation index is presented Table 8.

Confusion matrices, provide a clear view of numeric representation on incorrect and correct predictions. Figure 8 illustrates the neural network model's performance during the training stage, where it achieved an accuracy of 92.71% with an

Figure 6 Gradient descent curve (a) and validation loss (Val fail) (b)

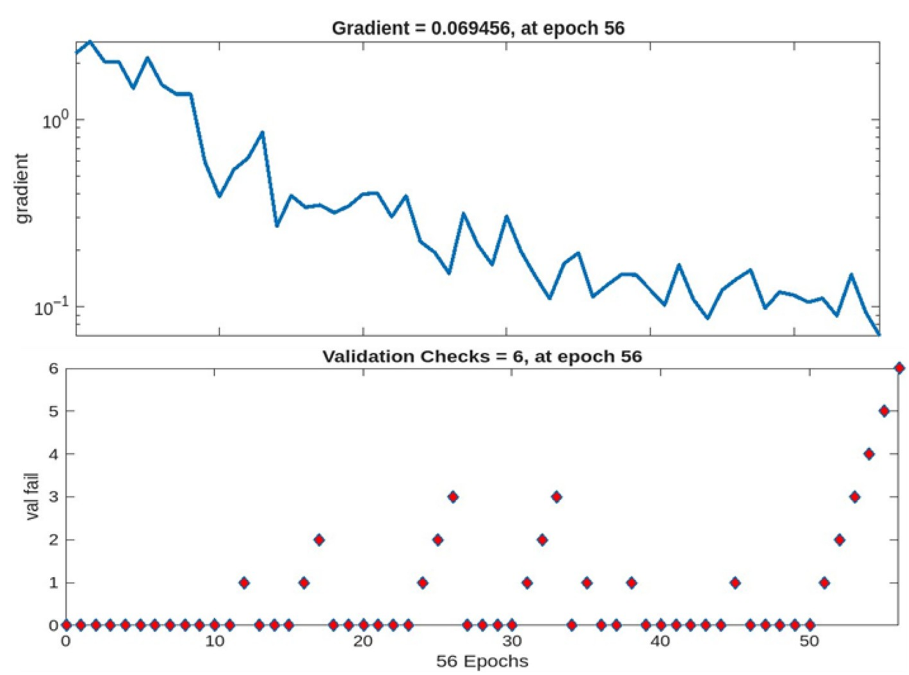

Source: Figure by authors

Figure 7 Training performance

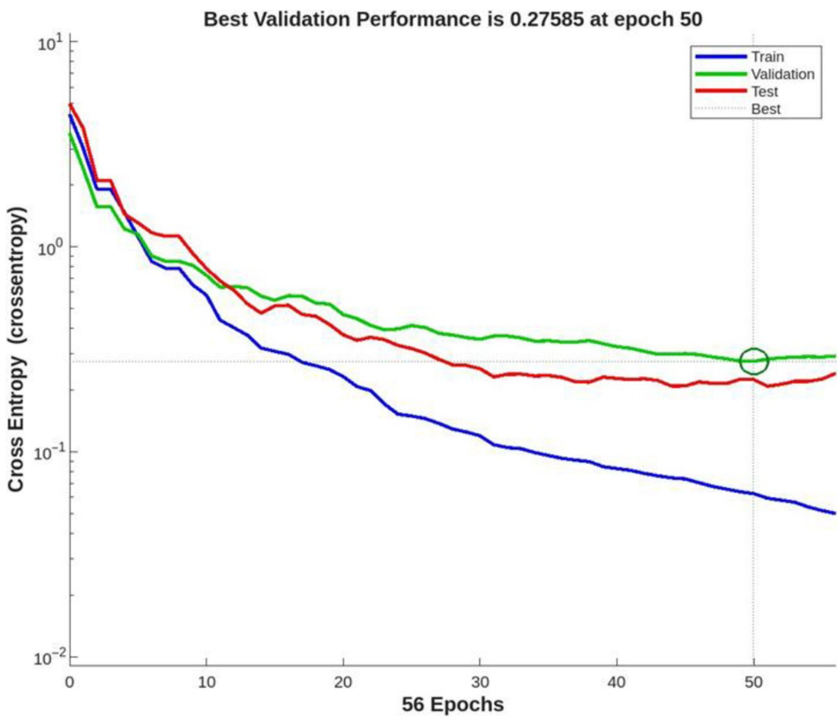

Source: Figure by authors

Table 8 Key performance metrics

Metric	Definition	Formula
True positive (TP)	Is the number of correctly predicted as class i	–
True negative (TN)	Is the number correctly predicted as non-class i	–
False positive (FP)	Is the number incorrectly predicted as class i,	–
False negative (FN)	Is the number incorrectly predicted as non-class i.	–
Accuracy	Proportion of correctly classified instances among all instances	(TP + TN)/(TP + TN + FP + FN)
Precision	Proportion of true positives among all predicted positives	TPi/(TPi + FP)
Recall (sensitivity)	Proportion of true positives correctly predicted	TPi/(TPi + FNi)
Specificity	Proportion of true negatives correctly predicted	TN/(TN + FP)
F1-score	Comprehensively considers accuracy and recall	2 × precision × Recalli/Precision + Recalli

Source(s): Table by authors

error rate of 7.3%. Within the training data set of 178 observations, the model demonstrated robust predictive capability, correctly identifying 149 out of 165 instances. Specifically, it accurately predicted 30 out of 35 no-rockburst observations, 39 out of 45 weak rockburst observations, 66 out of 68 moderate rockburst observations and 30 out of 30 strong rockburst observations.

The validation process refines hyperparameters and evaluates model performance using a separate data set to assess how well the model generalises to new data. This provides a comprehensive view of the model's robustness. The model achieved a validation accuracy of 76.3%. The test confusion matrix evaluates the trained model's ability to generalise to unseen data. The model achieved a test accuracy of 63.2%, indicating a drop in performance compared to the training and validation phases. The all-confusion matrix consolidates the model's performance across the training, validation and testing phases into a single matrix, providing a comprehensive overview of the model's effectiveness. The model achieved an overall accuracy of 85.8%, accurately predicting 218 out of 254 rockburst instances with very good performance rates across the different classes.

The overall prediction results are summarised per class in Table 9 and illustrated in Figure 8. Based on inner class results and overall performance Model 4 predicted with higher success Class «No" and Class: "Strong", whereas the model presents lower performance in Class: weak and Class: moderate rockburst, according to most of the metrics, across training validation, test. A comparison of the metrics suggests that F1-score and accuracy give more conservative scores.

Figure 8 Prediction results training confusion matrix; validation confusion matrix; test confusion matrix; all confusion matrix

Source: Figure by authors

6.1.1 Cross-validation and the ROC curve

Figure 9 illustrates the ROC curves for training, validation and testing phases and the overall ROC curve. The training ROC curve indicates the neural model's strong performance across all rockburst classes, with curves approaching the ideal upper left corner. The validation ROC curve reveals a slight decline in performance for each rockburst class, which is further reflected in the testing phase. Despite these variations, the overall ROC curve demonstrates that the model maintained good performance across all rockburst classes, indicating its robustness and reliability. The area under curve (AUC), ranges from 0 to 1, the larger the AUC stronger the classification. The macro-average AUC is 0.96, for all classes.

7. Discussion

Rockburst prediction is a problem that many researchers investigated in the last 50 years, as its of crucial importance to the design and construction of underground projects. In Zhou *et al.*, 2016 empirical criteria, (including Russenes (1974) criterion, the rock brittleness coefficient, Zhang *et al.* 2020), the strain energy storage index (Kidybiński 1981), were assessed in evaluating rock burst intensity prediction and the findings suggested, that the empirical methods could not generate satisfactory predictions for these cases as the predictive accuracy ranged between 20 and 51%.

This deficiency could be attributed to the fact that these criteria are mostly dependent on geomechanical parameters of the rock such as uniaxial compressive strength of the rock, as well as its tensile strength and elasticity modulus, while dynamic loads are not considered (Askaripour *et al.*, 2022).

It is important to take into consideration that rock bursting is strongly site-specific, depending on many factors such as the magnitude and direction of *in situ* stresses, the strength of the rock mass and the geometry of the excavation, blasting intensity, extraction rate as well as the applied excavation methods. Therefore, it is difficult to suggest universal and practical rockburst criteria Zhou *et al.* (2016).

The use of machine learning algorithms to assess the risk of rockbursts seems to be promising, but further investigation is needed. It is expected to improve the generalisation ability of the proposed models, and include factors, such as dynamic loading, the influence of construction disturbance, the size of the excavation, the amount of explosive charge and the support method used in construction (Askaripour *et al.*, 2022).

Table 9 Confusion matrix results, using metrics accuracy, precision, recall, specificity and F1-score

Class	Accuracy	Precision	Recall	Specificity	F1-score
Training					
No	0.959	0.857	0.938	0.964	0.895
Weak	0.949	0.867	0.929	0.955	0.897
Moderate	0.949	0.971	0.904	0.980	0.936
Strong	0.994	1.000	0.968	1.000	0.984
Validation					
No	0.921	0.889	0.800	0.964	0.842
Weak	0.895	0.714	0.714	0.935	0.056
Moderate	0.789	0.824	0.737	0.842	0.778
Strong	0.921	0.400	1.000	0.917	0.714
Test					
No	0.868	0.375	1.000	0.857	0.545
Weak	0.737	0.545	0.545	0.815	0.545
Moderate	0.763	0.786	0.647	0.857	0.710
Strong	0.895	0.800	0.571	0.968	0.667
Overall					
No	0.950	0.788	0.911	0.956	0.845
Weak	0.921	0.794	0.833	0.944	0.813
Moderate	0.912	0.919	0.835	0.957	0.875
Strong	0.973	0.900	0.900	0.984	0.900

Source(s): Table by authors

A large database of rockburst events from available databases, applying machine learning techniques, and subsequently confirm predictions with real rockburst events, might allow for the development of more accurate prediction methods for rockburst.

In the current study a datacentric long term rockburst intensity prediction for underground excavations is proposed applying multilayer perceptron (MLP) autoencoder model. The findings suggest that the best performing model based on the optimal feature combination, achieved an overall accuracy of 85.8%, accurately predicting correct 218 out of 254 rockburst instances across the different classes. The macro-average AUC is 0.96, and hight for all classes. However, it is important to note that while the training phase may yield impressive results, the model's performance during the validation and test phases might not be as strong. This is expected given the smaller data set allocated to these phases (15% for validation and 15% for testing). The algorithm has access to less data during these phases, which may limit its ability to generalise and accurately predict outcomes. Although it is expected that validation and testing results may be slightly less effective than the training, it is crucial to interpret these results with caution.

There are limitations in this approach that develop around that of lithology consideration, the small sized and imbalanced data set and black-box approach. Advanced deep learning

Figure 9 Training ROC; validation ROC; test ROC; all ROC

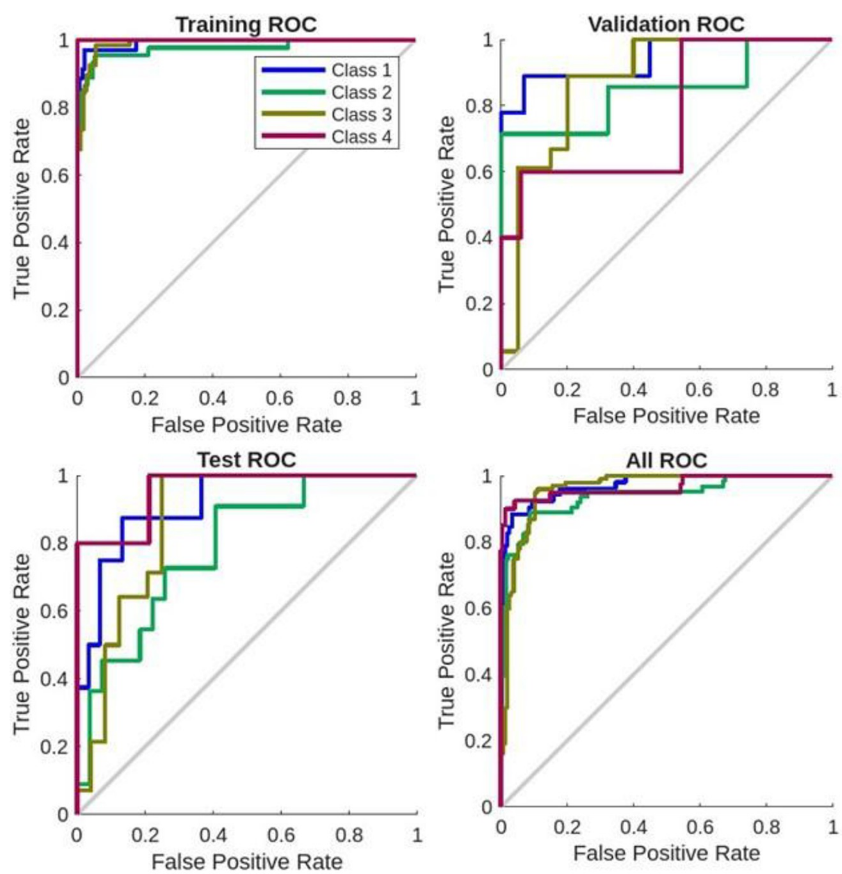

Source: Figure by authors

methods to adjust dynamically, sampling techniques and handle imbalanced data, could be a plausible pathway. Applying trained models in mining conditions, will be necessary to enhance model predictions.

It was also investigated in Ferentinou and Kayemberkn (2025), forthcoming that even though each rockburst case had an original corresponding label (rockburst intensity), it was not clear which rockburst intensity ranking criterion was adopted for the original classification. An unsupervised machine learning method (clustering) using self-organising maps, was introduced to investigate cluster tendency and seven decipherable clusters were identified. The rockburst cases based on their own attributes only were relabelled and after clustering, the prediction performance was 93.66%.

8. Conclusions

In this paper, a data set, including 254 rockburst instances, was compiled. An MLP autoencoder model is proposed, to predict long term rockburst intensity for underground excavations. The optimal feature combination was investigated, and the data split, percentage, between training and test sets. As a result, five models were developed and according to the findings rockbursts were best classified by the combination of the following parameters: tangential stress around underground opening (σ_θ), the uniaxial compressive strength, (σ_c), the uniaxial tensile strength, (σ_t); strain energy storage index (W_{ET}), brittle coefficients B1, B2. The applied data split was 70% training, 30% validation. The overall performance for all the models, was found to be 85.8%. On average, 63.2% of rockbursts in the test data sets were correctly classified. The models, predicted with higher success Class «No" and Class: "Strong", whereas the models presented lower performance in Class: "Weak" and Class: "Moderate", according to the majority of metrics, across training, validation, test and overall data sets.

It can be concluded that machine learning can better map the relationship between multiple highly nonlinear variables compared to the empirical rockburst prediction methods. The machine learning-based rockburst classification can improve the reduction of risk in underground excavations and mining environments and showed to have great potential through this data-driven approach.

References

Askaripour, M., Saeidi, A., Rouleau, A. and Mercier-Langevin, P. (2022), "Rockburst in underground excavations: a review of mechanism, classification, and prediction methods", *Underground Space*, Vol. 7 No. 4, pp. 577-607.

Bengio, Y., *et al.* (2007), "Greedy Layer-Wise training of deep networks", *Advances in Neural Information Processing Systems*, Vol. 19, pp. 153-160.

Blake, W. and Hedley Rockbursts, D.G (2003), "Case studies from North American Hard-Rock mines society for mining, metallurgy, and exploration (SME)".

Cai, M. (2024), "Rockburst risk control and mitigation in deep mining", *Deep Resources Engineering*, Vol. 1 No. 2, p. 100019.

Chen, L., Yang, X., Guo, L. and Yu, S. (2024), "Analysis of rock mass energy characteristics and induced disasters considering the blasting superposition effect", *Processes*, Vol. 12 No. 6.

Chen, L., Wu, S., Jin, A., Zhang, C. and Li, X. (2023), "Rockburst prediction and evaluation model for hard rock engineering based on extreme gradient boosting ensemble learning and SHAP value", *Geotechnical and Geological Engineering*, Vol. 41 No. 7, pp. 3923-3940.

Cortés, N., Hekmatnejad, A., Pan, P., Mohtarami, E., Pena, A., Taheri, A. and González, C. (2024), *Empirical Approaches for Rock Burst Prediction: A Comprehensive Review and Application to the New Level of El Teniente Mine*, Heliyon, Chile, *10*, p. e26515.

Dong, L-J., Li, X-B. and Peng, K. (2013), "Prediction of rockburst classification using random Forest", *Transactions of Nonferrous Metals Society of China*, Vol. 23 No. 2, pp. 472-477.

Du, K., Bi, R., Khandelwal, M., Li, G. and Zhou, J. (2024), "Occurrence mechanism and prevention technology of rockburst, coal bump and mine earthquake in deep mining", *Geomechanics and Geophysics for Geo-Energy and Geo-Resources*, Vol. 10 No. 1, p. 98.

Fan, L., Chang, Y., Peng, K., Bai, Y., Luo, K., Wu, T. and Ma, T. (2024), "Research progress on the mechanisms and control methods of rockbursts under water–rock interactions", *Applied Sciences*, Vol. 14 No. 19.

Feng, X., Chen, B., Li, S., Zhang, C., Xiao, Y., Feng, G., Zhou, H., Qiu, S., Zhao, Z., Yu, Y., Chen, D. and Ming, H. (2012), "Studies on the evolution process of rockbursts in deep tunnels", *J. Rock Mech. Geotech. Eng.*, Vol. 4, pp. 289-295, doi: 10.3724/sp.j.1235.2012.00289.

Hedley, D.G. (1987), *Rockburst Mechanics Canada Centre for Mineral and Energy Technology*, Ottawa, Australia.

Hu, J., He, M., Li, H., Tao, Z., Liu, D., Cheng, T. and Peng, D. (2024), "Rockburst hazard control using the excavation compensation method (ECM): a case study in the Qinling water conveyance tunnel", *Engineering*, Vol. 34, pp. 154-163.

Jia, Z.-C., Wang, Y., Wang, J.-H., Pei, Q.-Y. and Zhang, Y.-Q. (2024), "Rockburst intensity grade prediction based on data preprocessing techniques and multi-model ensemble learning algorithms", *Rock Mechanics and Rock Engineering*, Vol. 57 No. 7, pp. 5207-5227.

Jiang, B., Wu, K., Wang, Q., Wang, Y., Wu, W., Feng, Y. and Zhang, Y. (2025), "Dynamic damage characteristics and control mechanism of rocks anchored by constant resistance and energy absorption material", *International Journal of Mining Science and Technology*, Vol. 35 No. 1, pp. 57-67.

Kaiser, P.K., McCreath, D.R. and Tannant, D.D. (1996), *Canadian Rockburst Support Handbook: Prep. for Sponsors of the Canadian Rockburst Research Program 1990-1995*, Geomechanics Research Centre, p. 6.5.

Kidybiński, A. (1981), "Bursting liability indices of coal", *International Journal of Rock Mechanics and Mining Sciences and Geomechanics Abstracts*, Vol. 18, pp. 295-304.

Lei, W., Chai, J., Liu, J., Cao, Y., Yuchi, X., Zhang, D., Zheng, C., Du, X. and Gong, Y. (2025), "Research on stress release and pressure relief mechanism of underlying coal and rock under protective layer mining", *Scientific Reports*, Vol. 15 No. 1, p. 5583.

Li, H., Yang, Y., Zhang, Z. and Tang, L. (2025), "Prediction and classification technology of rockburst hazard in deep buried and high in-situ stress tunnel", *Scientific Reports*, Vol. 15 No. 1, p. 9633.

Li, M., Li, K., Qin, Q., Yue, R. and Shi, J. (2023), "Research and application of an intelligent prediction of rock bursts based on a Bayes-optimized convolutional neural network", *International Journal of Geomechanics*, Vol. 23 No. 5, p. 04023042.

Lin, S., Liang, Z., Dong, M., Guo, H. and Zheng, H. (2024), "Imbalanced rock burst assessment using variational autoencoder-enhanced gradient boosting algorithms and explainability", *Underground Space*, Vol. 17, pp. 226-245.

Luo, H., Fang, Y., Wang, J., Wang, Y., Liao, H., Yu, T. and Yao, Z. (2023), "Combined prediction of rockburst based on multiple factors and stacking ensemble algorithm", *Underground Space*, Vol. 13, pp. 241-261.

Lv, H., Cheng, Z., Xie, F., Pan, J. and Liu, F. (2024), "Study on hydraulic fracturing prevention and control of rock burst in roof of deep extra-thick coal seam roadway group", *Scientific Reports*, Vol. 14 No. 1, p. 29537.

Mahmoodzadeh, A., Ghazouani, N., Mohammed, A.H., Ibrahim, H.H., Alghamdi, A., Albaijan, I. and El Ouni, M.H. (2024), "Predicting rockbursts in deep tunnels based on ejection velocity and kinetic energy measurements using advanced machine learning", *Automation in Construction*, Vol. 166, p. 105671.

Miao, D., Kaixin, Y., Wenhao, W., Lu, L. and Sui, X. (2024), "Risk prediction of coal mine rock burst based on machine learning and feature selection algorithm", *Georisk: Assessment and Management of Risk for Engineered Systems and Geohazards*, Vol. 18 No. 4, pp. 868-881.

Moein, M.J.A., Langenbruch, C., Schultz, R., Grigoli, F., Ellsworth, W.L., Wang, R., Rinaldi, A.P. and Shapiro, S. (2023), "The physical mechanisms of induced earthquakes", *Nature Reviews Earth and Environment*, Vol. 4 No. 12, pp. 847-863.

Ortlepp, W.D. and Stacey, T.R. (1994), "Rockburst mechanisms in tunnels and shafts", *Tunnelling and Underground Space Technology*, Vol. 9 No. 1, pp. 59-65, doi: 10.1016/0886-7798(94)90010-8.

Pu, Y., Apel, D.B. and Xu, H. (2019), "Rockburst prediction in kimberlite with unsupervised learning method and support vector classifier", *Tunnelling and Underground Space Technology*, Vol. 90, pp. 12-18.

Qi, S., Guo, S., Waqar, M.F., Luo, G. and Zhang, S. (2024), "Prediction of brittle rock failure severity: an approach based on rock mass failure progress", *Journal of Rock Mechanics and Geotechnical Engineering*, Vol. 16 No. 12, pp. 4852-4865.

Ren, C., Sun, X., He, M. and Liu, D. (2025), "Experimental simulation investigation on slab buckling rockburst in deep tunnel", *Applied Sciences*, Vol. 15 No. 4.

Rong, H., Li, N., Cao, C., Wang, Y., Wei, S., Li, J. and Li, M. (2024), "A method for assessing the risk of rockburst based on coal-rock mechanical properties and In-Situ ground stress", *Scientific Reports*, Vol. 14 No. 1.

Russenes, B.F. (1974), "Analysis of rock spalling for tunnels in steep valley sides", Master thesis Norwegian Institute of Technology, Trondheim.

Salmi, E.F. and Sellers, E.J. (2021), "A review of the methods to incorporate the geological and geotechnical characteristics of rock masses in blastability assessments for selective blast design", *Engineering Geology*, Vol. 281, p. 105970.

Shan, L., Xiao, F., Liu, G. and Xie, K. (2024), "Research on the outburst–rockburst coupling disaster law based on true triaxial unloading tests", *Applied Sciences*, Vol. 14 No. 11.

Tian, X., Dou, L., Hu, S., Ma, X. and Lu, F. (2025), "Risk assessment and mechanism of rock burst for deep soft coal roadways", *Scientific Reports*, Vol. 15 No. 1, p. 7054.

Wang, Y., Xu, J. and Zhang, Y. (2025), "Dynamic numerical simulation analysis of rockburst grade evaluation based on rock mass strength", *Scientific Reports*, Vol. 15 No. 1, p. 7272.

Wang, K., He, B., Samui, P. and Zhou, J. (2024), "Predicting rock burst in underground engineering leveraging a novel metaheuristic-based LightGBM model", *Computer Modeling in Engineering and Sciences*, Vol. 140 No. 1, pp. 229-253.

Watson, J., Canbulat, I., Zhang, C. and Wei, C. (2025), "Energies within rock mass and the associated dynamic rock failures", *Rock Mechanics and Rock Engineering*, Vol. 58 No. 5, pp. 4935-4958.

Witkowski, W.T., Łucka, M., Guzy, A., Sudhaus, H., Barańska, A. and Hejmanowski, R. (2024), "Impact of mining-induced seismicity on land subsidence occurrence", *Remote Sensing of Environment*, Vol. 301, p. 113934.

Wojtecki, U., Bukowska, M. A., Iwaszenko, S. and Apel, D.B. (2024), "Machine learning-based classification of rock bursts in an active coal mine dominated by non-destructive tremors", *Applied Sciences*, Vol. 14 No. 12.

Wu, W., Gong, F. and Zhang, Z. (2024), "Sidewall rockburst characteristics of highly stressed circular tunnel under impact load", *Journal of Rock Mechanics and Geotechnical Engineering*, Vol. 16 No. 12, pp. 4909-4924.

Xia, Z., Mao, J. and He, Y. (2022), "Rockburst intensity prediction in underground buildings based on improved spectral clustering algorithm", *Frontiers in Earth Science*, Vol. 10.

Xu, Y. and Goodacre, R. (2018), "On splitting training and validation set: a comparative study of cross-validation, bootstrap and systematic sampling for estimating the generalization performance of supervised learning", *Journal of Analysis and Testing*, Vol. 2 No. 3, pp. 249-262.

Xu, G., Li, K., Li, M., Qin, Q. and Yue, R. (2022), "Rockburst intensity level prediction method based on FA-SSA-PNN model", *Energies*, Vol. 15 No. 14.

Zhang, Z., Luo, C., Zhang, H. and Gong, R. (2020), "Rockburst identification method based on energy storage limit of surrounding rock", *Energies 13*, doi: 10.3390/en13020343.

Zhou, J., Yang, P., Peng, P., Khandelwal, M. and Qiu, Y. (2023), "Performance evaluation of rockburst prediction based on PSO-SVM, HHO-SVM, and MFO-SVM hybrid models", *Mining, Metallurgy and Exploration*, Vol. 40, pp. 617-635.

Zhou, J., Li, X. and Mitri Hani, S. (2016), "Classification of rockburst in underground projects: comparison of ten supervised learning methods", *Journal of Computing in Civil Engineering*, Vol. 30 No. 5, p. 4016003.

Zhou, J., Li, X. and Shi, X. (2012), "Long-term prediction model of rockburst in underground openings using heuristic algorithms and support vector machines", *Safety Science*, Vol. 50 No. 4, pp. 629-644.

Zhou, J., Zhang, Y., Li, C., He, H. and Li, X. (2024a), “Rockburst prediction and prevention in underground space excavation”, *Underground Space*, Vol. 14, pp. 70-98.

Zhou, Y., Lv, W., Zhang, C., Zhou, Z., Wang, H., Liang, Q., Tang, Q., Han, G., Guo, W. and Zhao, D. (2024b), “Novel hard rock breaking technique using ultra-high-frequency particle impact induced by ultrasonic vibration field”, *Energy*, Vol. 288, p. 129747.

Further reading

Deng, J., Gong, Y. and Li, S. (2025), “Induced mechanism of tunnel rockbursts based on dynamic buckling of rock plates”, *Geohazard Mechanics*, Vol. 3 No. 1, pp. 15-27.

He, M., Cheng, T., Qiao, Y. and Li, H. (2023), “A review of rockburst: experiments, theories, and simulations”, *Journal of Rock Mechanics and Geotechnical Engineering*, Vol. 15 No. 5, p. 1312-1353.

Li, T., Ma, C., Zhu, M., Meng, L. and Chen, G. (2017), “Geomechanical types and mechanical analyses of rockbursts”, *Engineering Geology*, Vol. 222, pp. 72-83.

Tang, B. (2000), “Rockburst control using destress blasting”, *Thesis. Department of Mining and Materials Engineering*, McGill University, rj4306440.

Wang, C., Wu, A., Lu, H., Bao, T. and Liu, X. (2015), “Predicting rockburst tendency based on fuzzy matter–element model”, *International Journal of Rock Mechanics and Mining Sciences*, Vol. 75, pp. 224-232.

Wang, J., Apel, D.B., Pu, Y., Hall, R., Wei, C. and Sepehri, M. (2021), “Numerical modeling for rockbursts: a state-of-the-art review”, *Journal of Rock Mechanics and Geotechnical Engineering*, Vol. 13 No. 2, pp. 457-478.

Zeng, Y., Chen, J., Li, D. and Li, X. (2020), “Study on rock burst behavior and tendency identification of surrounding rocks in hard and brittle formations of deep and ultra-deep wells”, *IOP Conference Series: Earth and Environmental Science*, Vol. 570 No. 3, p. 032056.

Corresponding author

Maria Ferentinou can be contacted at: M.Ferentinou@ljmu.ac.uk